NATIONAL AERONAUTICS AND SPACE ADMINISTRATION

Technical Memorandum 33-607

Statistical Error Model for a Solar Electric Propulsion Thrust Subsystem

M. H. Bantell

JET PROPULSION LABORATORY

CALIFORNIA INSTITUTE OF TECHNOLOGY

PASADENA, CALIFORNIA

June 1, 1973

NATIONAL AERONAUTICS AND SPACE ADMINISTRATION

Technical Memorandum 33-607

Statistical Error Model for a Solar Electric Propulsion Thrust Subsystem

M. H. Bantell

JET PROPULSION LABORATORY
CALIFORNIA INSTITUTE OF TECHNOLOGY
PASADENA, CALIFORNIA

June 1, 1973

Prepared Under Contract No. NAS 7-100
National Aeronautics and Space Administration

PREFACE

The work described in this report was performed for the Mission Analysis Division by the Guidance and Control Division of the Jet Propulsion Laboratory.

CONTENTS

FIGURES (contd)

ABSTRACT

The Solar Electric Propulsion thrust subsystem statistical error model was developed as a tool for investigating the effects of thrust subsystem parameter uncertainties on navigation accuracy. The model is currently being used to evaluate the impact of electric engine parameter uncertainties on navigation system performance for a baseline mission to Encke's Comet in the 1980s.

The data given here represent the next generation in statistical error modeling for low-thrust applications. Principal improvements include the representation of thrust uncertainties and random process modeling in terms of random parametric variations in the thrust vector process for a multi-engine configuration.

I. INTRODUCTION

The use of continuous thrust for deep space missions presents navigation problems that are ordinarily nonexistent in ballistic missions. These problems arise from the presence of proportionately large random accelerations resulting from uncertainties in the thrust vector. Therefore, a principal concern in the study of thrust tolerance on navigation accuracy is the construction of a realistically adequate model and statistics for the expected behavior of the thrust variations.

In this report, a model for the covariance of random variations in the thrust vector is developed in terms of the parameters that affect thrust magnitude and pointing. Principal sources of error include the engines, thrust vector control and attitude control systems. Section II gives an overview development of the covariance equations and establishes a foundation for the technique employed. The structure of the covariance model is motivated in brief by summarizing some of the more important aspects of the propagation of the covariance of state in the presence of correlated acceleration (process) noise. In particular, it is shown that covariance propagation is greatly simplified by (1) the decoupling of the mapping from parameter space to state space and (2) the use of the Markov assumption in random process modeling. Section III summarizes the statistical model and presents a comparison of the results with covariance models used in previous low-thrust navigation studies.

In Sections IV to VII, the details of the calculations required to reach these results are presented. In particular, in Section IV, error models are developed relating parameter variations to thrust variations. The errors are discussed in terms of the physical processes that affect their absolute magnitude and variations as a function of time. The system covariance model is derived in Section V. The development considers a general class of error sources to be composed of a combination of independent and common errors.

Independent errors, by definition, do not share a common source, whereas common or additive errors are derived from a central source. It is shown that error sources must be differentiated in this fashion for a multi-engine configuration. The distinction is made because the effect of an independent source is reduced by averaging, whereas the effect of common sources is compounded by addition. The stochastic process for the random process variations is given in Section VI. Justification for the use of the Markov assumption is discussed in light of expected random behavior of the parameters. In Section VII, the error model parameters are classified in terms of independent and common sources. The covariance for the stochastic processes of parameter error sources are subsequently mapped by the error models to covariance for component thrust acceleration variations.

II. DYNAMICS OF STATE COVARIANCE PROPAGATION

In order to develop an understanding for the structure of the statistical model, it is helpful to establish perspective by presenting some of the aspects of the dynamics of covariance propagation. The basic considerations are simple enough to be understood without recourse to extensive development. Reference 1 provides an in-depth analysis of the subject.

The dynamics of the spatial state vector ($\bar{y}$) due to acceleration errors is given by a linear perturbation equation of the form

$$\left.\begin{aligned} \delta\dot{\bar{y}} &= B\delta\bar{y} + \delta\left(\frac{\bar{T}}{m}\right) \\ B &= \frac{\partial\bar{f}}{\partial\bar{y}} \end{aligned}\right\} \qquad (1)$$

where, along the nominal trajectory,

$$\dot{\bar{y}} = f(\bar{y}) + \frac{\bar{T}}{m}$$

and where $(\overline{T}, m)$ represent the nominal thrust and mass respectively. The rocket equation

$$T = \dot{m} v_e \qquad \text{(see the Appendix)}$$

is used to expand $\delta(\overline{T}/m)$ about a nominal point (0), resulting in the relation

$$\delta\left(\frac{\overline{T}}{m}\right) = \frac{T_0}{m_0}\left[\frac{\delta\overline{T}}{T_0} + \frac{\dot{m}t_0}{m_0}\left(\frac{\delta T}{T_0} - \frac{\delta v_e}{v_{e_0}}\right)\hat{T}_0\right]$$

where

$\dot{m}$ = propellant mass flow rate, assumed constant

v_e = exhaust velocity

$\hat{T}_0$ = unit vector in the direction of the nominal thrust

t_0 = time measured from launch

$m(t) = M - \int_0^t \dot{m}\, dt$, M = launch weight

For the worst-case condition at encounter,

$$\frac{\dot{m}t_0}{m_0} = \frac{m_p}{m_f} \approx 0.01$$

where

m_p = total propellant mass

m_f = spacecraft dry mass

The quantity $\delta v_e / v_{e_0}$ is on the order of $\delta T / T_0$ so that, to first order, the total effect of mass variation and uncertainty can be neglected. A linear mapping of thrust acceleration parameter errors to equivalent spacecraft thrust acceleration errors is given by

$$\delta\left(\frac{\overline{T}}{m}\right)_i = w_i = C_{ij}(N, \overline{x}_0)\, x_j \qquad \begin{matrix} i = 1,3 \\ j = 1,8 \end{matrix} \qquad (2)$$

where N is the number of operating thrusters in a multi-engine configuration and $\bar{x}_0$ is the vector of perturbations in the totality of parameters of the thrust vector process about some nominal value.[1]

Sufficient accuracy in the statistical description of the thrust process is obtained by assuming the thrust parameter errors to be generated by a first-order Gauss-Markov random process of the form

$$\dot{x}_i = \alpha_i x_i + \eta_i, \quad i = 1, 8 \tag{3}$$

where α_i is a constant for the process and η_i is white driving noise characterized by moments

$$E[\eta_i] = 0$$

$$E[\eta_i^2] = \sigma_{\eta_i}^2$$

The physical justification for the choice of this process will be given in Section VI.

The covariance matrix for the acceleration noise as a function of thrust process parameter noise is the covariance of Eq. (2):

$$R_w(t) = C\, R_x(t)\, C^T \tag{4}$$

Typically, an autocorrelation function is

$$R_{x_i}(t, \tau) = \sigma_{x_i}^2\, e^{-\alpha_i |t-\tau|}$$

[1] The eight components of the parameter vector are listed in Tables 1 and 2, where the rotational component due to star tracker errors has been neglected.

$$R_{x_i}(t) = \sigma^2_{x_i} \quad (t = \tau)$$

where $\sigma^2_{x_i}$ is the process variance.

The parameters $\bar{x}$ are assumed to be statistically independent to first order, and the mapping matrix C is such that the component thrust accelerations are uncoupled; i. e.,

$$C = \begin{bmatrix} [k_1, \cdots, k_5] & [0] \\ [0] & \begin{bmatrix} \ell_1 & 0 \\ 0 & \ell_2 \end{bmatrix} \end{bmatrix}, \quad \bar{x} = \left[\bar{x}_k, \bar{x}_\ell\right]^T$$

where the k's and ℓ's represent thrust magnitude and thrust pointing sensitivities respectively. These simplifications are physically justifiable and reduce the complexity of computing the covariance for the process noise and the consequent propagation in the covariance of state errors. This effect is shown by the following calculations.

Due to the nature of C and the assumed statistics of $\bar{x}$, it follows that the autocorrelation matrix for thrust acceleration errors must be of the form

$$R_{w_{ii}}(t, \tau) = \sigma^2_{w_i} e^{-\alpha_i |t-\tau|}, \quad i = x, y, z$$

with

$$R_{w_{ij}}(t, \tau) = 0 \text{ for all } i \neq j \tag{5}$$

where

$$\sigma^2_{w_x} = \Sigma k_i^2 \sigma^2_{k_i}, \; i = 1, 6$$

$$\sigma^2_{w_{y,z}} = \Sigma \ell_i^2 \sigma^2_{\ell_i}, \; i = 1, 2$$

Through the use of Eqs. (5), random processes for thrust acceleration errors can be constructed of the form

$$\dot{\overline{w}} = A\overline{w} + \overline{\xi} \tag{6}$$

where

$$A_{ij} = \alpha_i \begin{cases} i = j = x, y, z \\ 0 \text{ otherwise} \end{cases}$$

and $\overline{\xi}$ is the vector of white driving noise characterized by

$$\left.\begin{aligned} E[\xi_i] &= 0 \\ E\left[\xi_i^2\right] &= \frac{\sigma_{w_i}^2}{2\alpha_i} = Q_{ii} \end{aligned}\right\} \tag{7}$$

The state of the spacecraft is considered to be optimally determined by filtering the observables (measurements) in accordance with the minimization of some cost function, e.g., weighted least squares, minimum variance, etc. A required input to the algorithm is the propagation in the covariance of state due to the corruption by the covariance of acceleration noise $\overline{w}(t)$.

The propagation in the covariance matrix of state errors is found by the solution of the first-order matrix differential equation derived from Eqs. (1), (6), and (7):

$$\frac{dZ}{dt} = MZ + ZM^T + S$$

$$Z(0) = Z_0$$

where

$$z = [\overline{y}, \overline{w}] \text{ (9 vector)}$$

$$Z = E[\overline{z}\,\overline{z}^T] \text{ (9 } \times \text{ 9)}$$

Parameter matrices S and M are given by

$$S = \begin{bmatrix} (0) & (0) \\ \hline (0) & Q \end{bmatrix} \quad M = \begin{bmatrix} B & (0) \\ \hline (0) & A \end{bmatrix} \quad (9 \times 9)$$

III. SUMMARY

A. Strategy

Previous navigation studies of continuous thrust applications have invoked the Markov assumption. However, the resulting autocovariance matrix of thrust acceleration errors was assumed to be spherically distributed, of the form

$$R(t, \tau) = \sigma_w^2 \, e^{-\alpha|t-\tau|}[I] \quad (3 \times 3) \tag{8}$$

where σ_w^2 is the process variance. The selection of values for the model parameters (σ_w^2, α) were usually made by physical intuition and independent of any considerations of thrust parameter variations.

Although the simplified model given by Eq. (8) is tractable and possesses a certain degree of physical justification (Ref. 2), the parameters of the model fail to correlate uncertainties in thrust to uncertainties in the dominant thrust subsystem parameters and the factors that influence them. To overcome this deficiency, knowledge of dominant error sources that contribute to thrust magnitude and pointing error was obtained by investigating the composition of the component parts of the thrust system and all related subsystems, i. e., attitude and thrust vector control.

A realistic statistical (covariance) model is therefore achieved by meeting the following general objective: to specify the parameters of the model given by Eqs. (5), i. e., $(\sigma, \alpha)_{x, y, z}$ in terms of the totality of parameters $(\bar{x}_k, \bar{x}_\ell)$ that contribute to errors in the thrust vector. This objective is accomplished by the following approach:

(1) Define a hardware model for the thrust system and all related system functions.

(2) Derive a perturbation model relating changes in thrust in terms of engine parameter and related errors.

(3) Translate expected random behavior of parameter variations into statistical variables.

(4) Map statistics of parameter variations into statistics for thrust variations using the thrust perturbation model.

B. Results

The behavior of the standard deviations for the normalized components of $R_w(t, \tau)$, that is, $\sigma_w(x, y, z)$ in percent as a function of time, is shown in Fig. 1; component autocorrelations are stated in Eq. (15). These data comprise a compilation of thruster performance data presented in Table 1 and celestial reference data presented in Table 2. Standard deviation σ_{w_x} is shown to be directly proportional to $1/\sqrt{N}$ and hence follows the power curve. Switching points were based on an 18-kW thrust system with six operating thrusters. Equal throttling of all operating thrusters was presumed, with a maximum throttling constraint of 50% (see Fig. 2b). Standard deviations $\sigma_{w_{y,z}}$ do not follow the $1/\sqrt{N}$ law directly because of the contributions from $\sigma_{\epsilon_{y,z}}$ where $\bar{\epsilon}$ represents the vector of celestial reference errors mapped to spacecraft body coordinates.

C. Conclusions

Conclusions are as follows:

(1a) The standard deviation of the thrust magnitude σ_{w_x} is a root sum square of the uncertainty in the totality of parameters that regulate nominal thrust production (see Table 1). The variation in σ_{w_x} with time is attributed to the fact that all independently derived error sources vary as $\sqrt{N}$ on the basis of total thrust (ΔT_0) and decrease in proportion to

$$\frac{\sqrt{N}}{N} = \frac{1}{\sqrt{N}}$$

on the basis of percentage change in total thrust ($\Delta T / T_0$).

(1b) The maximum value of σ_{w_x} is 3.5%, which represents a factor of 3.5 increase in the value of σ_{w_x} (1.0%) for current process noise models in interplanetary flight. Launch and near-encounter values of σ_{w_x} approach the value for current models.

(2) The standard deviations for $\sigma_{w_{y,z}}$ fluctuate about the 1.0% level on the average and represent the uncertainty in thrust pointing. These errors are due to the mechanization of the celestial reference σ_ϵ and thruster misalignment σ_β. Thruster misalignments are independently derived, whereas celestial reference errors share a common source. Hence celestial reference errors will accumulate in proportion to N on the basis of total thrust (ΔT_0) but will be independent of the number of operating thrusters on the basis of percentage change in thrust.

(3) Attitude control limit cycling contributes a negligible amount (less than 0.05%) to thrust pointing uncertainty. This is due primarily to the continuous nature of the attitude control; the engine cluster (see Fig. 2a) is translated and two of the engines are rotated to maintain near-zero position error about the center of mass relative to the celestial reference. Limit cycling occurs due to backlash in the translator actuator and has a correlation time of hours. However, neglecting the contribution from attitude control, correlation times for all significant components of the acceleration process noise is on the order of weeks.

This result is contrasted with previous process noise models which have correlation times for pointing error on the order of hours. This assumption reflected the time variation associated with the normal period of oscillation of a typical Mariner-type deadband attitude control system.

Consideration of short correlation times is particularly important because variations on the order of hours tend to corrupt ground-based data types whose normal variations are proportional to the Earth's rate of rotation.

Hence it is concluded that angular acceleration process noise from a linear attitude control system should not have a detrimental effect on ground-based data types.

IV. ERROR MODELS

A. Definition of Fundamental System Functions

The model for the fundamental system of thrust vector error sources is shown in Fig. 2a. The thrust system receives conditioned solar power from N power conditioner units. The thruster array is composed of N operating thrusters and M spares (a five-thruster array; one spare is shown without loss of generality). The switching network couples the power conditioner units to the thrusters so that all operating thrusters are connected to separate power conditioner units.

Attitude and thrust vector control (TVC) are achieved simultaneously by means of a 2-degree-of-freedom translator mechanism. Control about the third axis normal to the plane of translation is achieved by differentially gimballing two of the engines. The TVC mechanism is actuated in discrete steps by means of a stepper motor. Attitude control is maintained by acquiring celestial references--traditionally, the Sun and a convenient reference star. Sensors used to implement the celestial reference system are two single-axis Sun sensors and a star tracker.

B. Thrust Subsystem

Before proceeding to the development of the error model for the thrust subsystem, a brief description of an electrostatic thruster is given in order to promote a qualitative understanding of the physics of electric propulsion. A typical thruster is shown in Fig. 3. Thrust is produced by the electrostatic acceleration of heavy charged particles (mercury ions) through a large potential V_B (typically, 3 kV), according to the "rocket equation" (see the Appendix, Section I):

$$\overline{T} = \dot{m}\overline{v}_e$$

where $\dot{m}$ is the mass flow rate of mercury (Hg) and $\overline{v}_e$ is the exhaust velocity of the ions relative to the spacecraft.

The ions are formed by the following process, known as electron bombardment. A source of electrons is provided by introducing mercury into the cathode vaporizer C. A baffle prevents high-energy electrons from being injected directly into the plasma. The low-energy electrons escape from

the cathode cavity and are accelerated toward the anode, which is maintained through closed-loop regulation at voltage V_d. The electrons spiral outward on the magnetic field lines, thus enhancing the ionization efficiency by permitting a single electron to make many collisions with neutral Hg atoms in traversing its path to the anode.

Mercury atoms are provided by introducing liquid Hg into the main vaporizer M. The flow rate of Hg is regulated by sensing the current drawn by the screen and accelerator grid power supplies (V_s, V_a) since $\dot{m}$ is directly proportional to the current drawn by the main beam I_B (see the Appendix, Section II). The exhaust plume is neutralized by injecting electrons directly into the exit beam.

The plasma consists of electrons, singly and doubly ionized mercury Hg^{+} and Hg^{++}, and neutral atoms Hg^{0}. The geometry of the electrostatic field lines is always such that the particles at the plasma interface removed from the center of the beamlet diverge as they exit into the exhaust plume (Fig. A-2). The resulting divergence causes a thrust degradation per beamlet proportional to the cosine of the average value of the divergence angle across the beamlet.

The nominal thrust from a single thruster is given by the relation (see the Appendix, Section II).

$$T = K\left(\frac{\eta_1 + \sqrt{2}\,\eta_2}{\eta_1 + 2\eta_2}\right) I_B \sqrt{V_B}\,(\overline{\cos\theta}\cos\beta)\zeta$$

where

$K = \sqrt{\frac{2m_0}{e}}$

m_0 = mass of atomic mercury (3.34×10^{-25} kg)

e = electronic charge unit (1.6×10^{-19} coulomb)

I_B = ion current in the exhaust beam = $(\eta_1 + 2\eta_2)\frac{e}{m_0}\dot{m}$

$\dot{m}$ = mass flow rate (kg/s)

V_B = net ion acceleration potential

η_1, η_2 = mass fraction of the total flow rate existing as singly and doubly charged mercury atoms, respectively

$\overline{\cos\theta}$ = exhaust beam divergence factor, abbreviated $\bar{c}_\theta$

ζ = thrust recovery factor = $1 + \epsilon$

β = accelerator and/or screen warpage and misalignment angle

Normalized perturbations in the thrust vector can be written in the convenient form

$$\frac{\Delta\overline{T}}{T} = \frac{1}{T}\left[\frac{\partial\overline{T}}{\partial\bar{x}}\Delta\bar{x} + \frac{\partial\overline{T}}{\partial\bar{\beta}}\Delta\bar{\beta}\right] \tag{9}$$

where T is the magnitude of the thrust and, nominally,[2] $\overline{T} = T_x \hat{x}$. The appropriate partial derivatives, when substituted into Eq. (9), provide

$$\left.\begin{aligned} K &= \frac{1}{T}\frac{\partial\overline{T}}{\partial\bar{x}} = \left[1,\ \frac{1}{2},\ k\left(\frac{\eta_2}{\eta_1}\right),\ -k\left(\frac{\eta_2}{\eta_1}\right),\ 1,\ \epsilon_0\right] \\ k &= 2 - \sqrt{2} \\ L_\beta &= \frac{1}{T}\frac{\partial\overline{T}}{\partial\bar{\beta}} = \begin{bmatrix} 0 & 1 \\ -1 & 0 \end{bmatrix} \\ \bar{x} &= \left[\frac{I_B}{I_{B_0}},\ \frac{V_B}{V_{B_0}},\ \frac{\eta_1}{\eta_{1_0}},\ \frac{\eta_2}{\eta_{2_0}},\ \frac{\bar{c}_\theta}{\bar{c}_{\theta_0}},\ \frac{\epsilon}{\epsilon_0}\right]^T \\ \bar{\beta} &= \left[\beta_x,\ \beta_z\right]^T \end{aligned}\right\} \tag{10}$$

where the subscript (0) refers to the nominal value of the parameter.

[2] $\hat{x}$, $\hat{y}$, $\hat{z}$ are the vehicle-body-axis coordinate system of unit vectors where x passes through the centroid of the exhaust plume and y is aligned with the solar panels, as shown in Fig. 2a.

The following summary data (Ref. 3) represent current knowledge of the uncertainties and contributing factors concerning the parameters given in Eqs. (10):

(1) V_B is the net potential difference experienced by the ions formed in the thruster from their point of formation to their point of departure from the spacecraft field of influence. This voltage will be uncertain to within about 4 V because of varying line drops and uncertainties in the thruster plasma potential and the ion beam exit potential. An additional voltage uncertainty is caused by the regulation of the main beam power supply. For the present units, this is 1%, or 20 V. The combination of these two factors gives an uncertainty of about 0.5% in the thrust and the specific impulse.

(2) I_B is the difference between the currents drawn by the main beam and accelerator power supplies and is the main control parameter for regulating thrust. Uncertainties in I_B arise primarily from the gain of the control loop, which regulates I_B, and from the drift in the reference that sets I_B. Present regulation schemes use type 0 controllers. The uncertainty introduced by the finite gain of the control loop coupled with the uncertainty in main vaporizer characteristics is on the order of 0.5 to 1%. Also, I_B is set by an analog reference signal against which the measured value of I_B is compared. Electronic components used to generate analog signals are subject to thermal and time-dependent drifts, which, if uncompensated, can result in an error of several percent. With reasonable compensation schemes, it is felt that this reference drift can be held to about 1%. Thus the total uncertainty in I_B is estimated to be on the order of 1.5% rss.

(3) The electrostatic and mechanical geometries of the accelerating structure produce an ion beam composed of many hundreds of small, diverging beamlets. The angle of divergence of the individual beamlets varies across the exit grid and also varies in time as a function of the beam current density. Because of the difficulty in measuring an individual beamlet, no precise

information is available on the true average beam-divergence loss. Faraday probe measurements in the ion beam are generally used to estimate the angle of divergence, but the errors in translating these measurements into a value of cos θ are probably large. Current estimates of Faraday probe data will not give the divergence angle to better than ±5 deg. The error or uncertainty that this introduces is obviously a function of the angle, which, in turn, is dependent on the electrostatic geometry. In general, divergence will increase with reduced specific impulse; it could vary from about 15 deg at 2 kV screen potential to up to 20 deg at 1 kV. It is estimated that, at 3000 s, the inherent uncertainty in the value of cos θ will be about $\pm 3\%$ around a base value of 0.96, and that cos θ will vary with I_B, with the magnitude of this variation at present unknown.

(4) The factor ζ is introduced to account for charge exchange and erosion effects. Examination of thruster accelerator grids indicates that most charge exchange ions originate downstream of the accelerator grid. The fast neutrals formed in the process then exit with a velocity higher than that of the ions, because they have not been decelerated through the full deceleration potential. This represents a slight thrust enhancement. A further small thrust enhancement is obtained by the release of material from the accelerator grid because of the charge exchange ion impact.

(5) By far the most important factors contributing to subsystem performance uncertainties are those affecting the mass flow rate. Because at present no direct measurement of mass flow rate is available, it must be controlled from some a priori calibration. Present control schemes utilize the relationship between the discharge power and the mass utilization efficiency (as indicated by the ion beam) at constant flow rate to regulate propellant flow. This implies that an a priori calibration of $(\eta_1 + \eta_2)$ versus P_{TH} (conditioned power delivered to the input terminals of a single thruster) and a subsidiary calibration of η_2 versus V_d (arc discharge voltage) are made. In flight, P_{TH} and V_d are controlled, and η_1 and η_2 are assumed to follow the calibration curves.

The difficulty with this scheme is the sensitivity of the calibration to a number of thruster parameters, including thruster geometry, magnetic field strength and geometry, division of flow between main and cathode vaporizers, cathode-keeper potential, total extraction voltage, and neutralizer coupling potential. These parameters will vary in time as a function of component aging, line and load variations, and subsystem random perturbations. Using present control schemes, the uncertainty in the initial calibration is probably on the order of 1%, and the variation in time on the order of ±5%.

(6) The angle β represents the achievable alignment accuracy of the thrust vector to the nominal thrust direction. This accuracy is a function of mechanical tolerances and the thermal load unbalance on the accelerating grids. No accurate measurements of β are available. However, a careful design should render β less than 2 deg (3σ). Current data indicate that β is time-invariant, implying that the grid plates warp to some maximum angles and attain a permanent set over the power profile. For the purpose of this study, β is considered time-varying with long correlation time.

(7) Thrust vectoring (gimballing) two of the thrusters (see Fig. 2a) reduces the net thrust in proportion to the cosine of the gimbal angle δ; the maximum gimballing angle is ±10 deg. Because the thrusters are used to achieve closed-loop attitude control, no a priori prediction of the vectoring loss can be made. However, δ is not modeled as a random variable in the thrust error equation because it is assumed that the gimbal angles will be calibrated and measured to an accuracy such that the resulting error in thrust will be less than 0.10%. Table 1 summarizes the current best estimates of the various error sources and their expected behavior as a function of time in accordance with the assumed process noise model.

C. Celestial Reference Error Model

Thrust pointing error caused by errors induced in mechanization of the celestial reference system can only be estimated in an order-of-magnitude sense at this time because sensor mechanization and strategy for acquiring the celestial reference have not been established. However, the following considerations indicate a probable approach to be taken.

Ballistic missions in the ecliptic plane require a star tracker with aperture-center axis normal to the vehicle roll axis. Consequently this axis is directed toward the south ecliptic pole. Since Canopus is the brightest star near this location, it is used for roll reference. However, for deviations from ecliptic flight, the large solar arrays can inhibit the field of view because the axis of the solar panels is constrained to be normal to the Sun line for the chosen baseline mission; gross rotations of the vehicle about an axis tangent to the plane of the orbit thus render Canopus viewing impossible during certain portions of the trajectory. The solution of the attitude reference problem will possibly involve any one or all of the following considerations: electrical and/or mechanical gimballing of the star tracker, use of multiple reference stars, and Sun-sensor gimballing because of the need for solar-panel articulation. A simplified analysis of thrust pointing error caused by celestial reference mechanization is presented here in lieu of any design data concerning the above technique(s).

It is assumed that the celestial reference system utilizes the Sun and a convenient reference star. The Sun sensors collectively have the equivalence of a two-axis sensor. Consequently, uncertainties in the Sun-sensor output trace a solid angle as shown in Fig. 4. The star tracker is sensitive to motion about or out of a plane. Therefore, uncertainties in the star-tracker output trace a wedge.

It is also assumed that $(\bar{\epsilon}_1, \bar{\epsilon}_2)$ and $\bar{\epsilon}_3$ represent small rotation vectors derived from errors in the Sun sensor and the star tracker respectively. In terms of percentage change in a single thrust vector normal to $\bar{T}$,

$$\frac{\Delta \bar{T}}{T} = \frac{1}{T} \frac{\partial \bar{T}}{\partial \bar{\epsilon}} \Delta \bar{\epsilon}$$

where

$$L_\epsilon = \frac{1}{T}\frac{\partial \overline{T}}{\partial \overline{\epsilon}} = \begin{bmatrix} 0 & -\sin\psi_\odot \\ 1 & 0 \end{bmatrix} \tag{11}$$

$$\overline{\epsilon} = [\epsilon_y, \epsilon_z]$$

Pointing error ϵ_y, ϵ_z can be determined using Sun-sensor errors only because the drift represents the dominant component of the angular uncertainty from a statistical point of view. Sensor biases and/or null offsets can be estimated in flight quite easily. However, the increase in knowledge of the average behavior of the random time-varying component is very slight. Nevertheless, the ability to estimate the state of the random process is increased as the correlation time becomes large. Sun-sensor errors are specified in the coordinate system defined by $\hat{x}'$, $\hat{y}'$, $\hat{c}$, as shown in Fig. 4. The inclusion of star-tracker errors in the model gives rise to thrust cross-correlation terms in y and z. However, the effect is probably negligible under the given set of assumptions concerning star-tracker drift as shown below.

Table 2 summarizes current estimates of Sun-sensor and star-tracker errors and their expected behavior as a function of time.

D. Thrust Vector Control

It has been shown that closed-loop operation of the thrust vector control system results in a low-frequency, low-amplitude limit cycle in each axis of the control system. This oscillation is a function of the electronic compensation time constants and the amount of backlash in the gimbal and translator actuators.

Laboratory tests have been run to show the effects of a worst-case actuator backlash on the system. Table 3 summarizes the results (see Ref. 4). Conclusions from the laboratory tests, taken from Ref. 4, are:

(1) Excessive actuator backlash causes an excessive number of step motor pulses in the closed-loop control system. Assuming that the total number of lifetime pulses allowed is 10^7, it is necessary to limit the pulses to one every 3 s on the average. The six-step

case shown in Table 3 promotes 20 pulses per cycle, which is excessive in terms of lifetime considerations.

(2) Small-amplitude, low-frequency oscillations are to be expected in each axis of the thrust vector control systems. The oscillations are so small in amplitude (less than ~0.005 deg peak to peak) that no noticeable effect in thrust vector pointing accuracy will be observed.

(3) The mechanization of the actual hardware shows a reduction in the total number of step motor pulses by a factor of 3, when compared to computer simulations of the control system limit cycle behavior.

On the basis of the preceding data, it is concluded that thrust pointing error caused by thrust-vector-control mechanization errors is negligible, under the stipulation that contributions to thrust pointing error of less than 0.05% are neglected. This criterion also considers the correlation time with equal weight, since variations on the order of hours tend to corrupt ground-based data types whose normal variations are proportional to the Earth's rate of rotation.

V. SYSTEM COVARIANCE MODEL

Variations in the net thrust vector with respect to a set of reference body coordinates are considered to occur from two processes: (1) changes in the nominal thrust in body coordinates and (2) rotations of the body coordinate system. Further classification of the error sources in a statistical sense provides data concerning the correlation of random variables. Errors of a specific type (i.e., voltage, current, etc.) which do not share a common source will be independent in a statistical sense, resulting in a root-sum-square net contribution. Conversely, an error that shares a common source will be perfectly correlated in a statistical sense, resulting in a summation of the contributions of the errors individually. However, the collection of all thrust parameter variables is assumed to be statistically independent to first order.

Symbolically,

$$W_i = \sum_{k=1}^{N} \sum_{j=1}^{M} A_{ijk} \lambda_{jk} + \sum_{k=1}^{N} \sum_{j=1}^{L} B_{ijk} \gamma_j$$

for each component W_i of the normalized thrust error vector in the reference coordinate system. The summations are carried out over the total number of operating thrusters N, the number M of independent errors λ_j, and the number L of common errors γ_j. In vector formulation, the thrust error is

$$\overline{W} = \sum_{i=1}^{N} A_i \overline{\lambda}_i + \sum_{i=1}^{N} B_i \overline{\gamma} \tag{12}$$

where, to first order in the errors,

$$A = \frac{1}{T_0} \frac{\partial \overline{T}}{\partial \overline{\lambda}}, \quad B = \frac{1}{T_0} \frac{\partial \overline{T}}{\partial \overline{\gamma}}$$

and where $\overline{T}(t)$ is the nominal thrust vector per thruster, and T_0 is the total thrust. Normalized random errors $\overline{\lambda}$ and $\overline{\gamma}$ assume the general form

$$\overline{\lambda}_i = \overline{\lambda}_{0_i} + \overline{\lambda}_i(t)$$

$$\overline{\gamma}_i = \overline{\gamma}_{0_i} + \overline{\gamma}_i(t)$$

where $\overline{\lambda}_{0_i}$, $\overline{\gamma}_{0_i}$ are biases and $\overline{\lambda}_i(t)$, $\overline{\gamma}(t)$ are time-varying components. It is assumed that the magnitude of the error is not a function of thrust and that bias and time-varying components are independent.

It has been assumed that the probable behavior of a single engine is representative of the engine cluster as a whole. This assumption provides a

great computational savings because only the average response of the navigation process to a representative set of uncertainties in the thrust process need be investigated. The assumption of statistical independence for the elements of the random parameter vectors $\bar{\lambda}$ and $\bar{\gamma}$ is entirely justifiable for normal operating conditions.

The autocovariance matrix is the expected value of Eq. (12) at arbitrary times t_1 and t_2:

$$R_w(t_1, t_2) = \sum_{i=1}^{N} A_i \, E\left[\bar{\lambda}_i(t_1)\, \bar{\lambda}_i^T(t_2)\right] A_i^T$$

$$+ \sum_{i=1}^{N} B_i \, E\left[\bar{\gamma}(t_1)\, \bar{\gamma}^T(t_2)\right] \sum_{i=1}^{N} B_i^T \qquad (13)$$

Define

$$\Lambda_i(t_1, t_2) = E\left[\bar{\lambda}_i(t_1),\ \bar{\lambda}_i^T(t_2)\right]$$

$$\Gamma(t_1, t_2) = E\left[\bar{\gamma}(t_1),\ \bar{\gamma}^T(t_2)\right]$$

where

$$E\left[\lambda_{ij}\, \lambda_{ik}^T\right] = 0,\ j \neq k$$

$$E\left[\gamma_i\, \gamma_j\right] = 0,\ i \neq j$$

Equal throttling of all operating thrusters is assumed, so that the mapping matrices A and B remain invariant from thruster to thruster ($T_0 = NT$), where

$$A_{(1)}, B_{(1)} = NA, NB$$

Finally, it is assumed that the autocovariance for the λ_{ij} are identical in agreement with a previous assumption, so that

$$\Lambda_i = \begin{bmatrix} R_{\lambda_1}(t_1, t_2) & & (0) \\ & \ddots & \\ (0) & & R_{\lambda_M}(t_1, t_2) \end{bmatrix} \text{for all } i = 1 \cdots N$$

Similarly, the autocovariance for the correlated error sources is

$$\Gamma = \begin{bmatrix} R_{\gamma_1}(t_1, t_2) & & (0) \\ & \ddots & \\ (0) & & R_{\gamma_L}(t_1, t_2) \end{bmatrix}$$

Equation (13) takes the form

$$R_w(t_1, t_2) = \frac{1}{N} A_{(1)} \Lambda(t_1, t_2) A_{(1)}^T + B_{(1)} \Gamma(t_1, t_2) B_{(1)}^T \qquad (14)$$

The preceding calculations indicate that all independently derived error sources ($\bar{\lambda}$) increase in proportion to $\sqrt{N}$ on the basis of total thrust ΔT and decrease in proportion to $\sqrt{N}/N = 1/\sqrt{N}$ on the basis of percentage change in total thrust $\Delta T/T_0$. Common errors $\bar{\gamma}$ add in proportion to N on the basis of total thrust and contribute the same amount on the basis of percentage change.

VI. STOCHASTIC PROCESS CONSIDERATIONS

Choosing a random process to adequately represent the stochastic behavior of the thrust and related system parameters is difficult because of the lack of any statistical data derived by experimentation. Meaningful experiments are virtually impossible because of the long correlation times involved.

In lieu of this data, some intuitive assumptions about $\lambda_i(t)$ must be made. It is desirable that $\lambda_i(t)$, $\gamma_i(t)$ possess the following properties (Ref. 5):

(1) The process should possess a unimodal probability density function. This implies that small values of the noise are expected to occur more often than large values.

(2) The process should be unbiased; i. e., the statistical average of the noise should tend to zero.

(3) The process should be autocorrelated in time. This is necessary because dominant variations in the process behavior are expected to occur at frequencies within the bandwidth defined by the characteristic frequency of the spacecraft dynamics.

(4) The process should be stationary. This implies that the variance of the noise is expected to remain constant in time.

A process which fits the preceding description was introduced by Ornstein and Uhlenbeck (Ref. 5) as a model for the velocity of a particle undergoing a Brownian motion. The statistical properties of the Ornstein-Uhlenbeck (O. U.) process are defined by the following relations:

(1) The probability density function is unmodal:

$$f[x(t)] = \frac{1}{\sqrt{2\pi}}\ \sigma_x\ e^{-1/2[x(t)/\sigma]^2}$$

where σ_x is the standard deviation of the process.

(2) The O. U. process is unbiased:

$$E[x(t)] = 0$$

(3) The O. U. process is exponentially autocorrelated in time:

$$R_x(t_1, t_2) = \sigma_x^2\ e^{-\alpha|t_2 - t_1|}$$

where $1/\alpha$ is the correlation time of the process and, since $R_x(t_1, t_2)$ depends only on the time difference $(t_2 - t_1)$, $x(t)$ is stationary.

There exists a duality between the continuous Gauss-Markov process and the O. U. process because both processes satisfy a Langevin equation of the form

$$\dot{x}(t) = \alpha X(t) + u(t)$$

where u(t) is Gaussian white noise, i. e.,

$$E[u(t)] = 0$$

$$R_u(t_1, t_2) = Q\,\delta(t_2 - t_1)$$

VII. COVARIANCE MAPPING

Covariance data for the thrust system and celestial sensors are mapped into covariance for percentage change in thrust $\Delta T/T$ by Eq. (14). The parameter transformation matrices A and B are

$$A_{(1)} = \left[\begin{array}{c|c} K & (0) \\ \hline (0) & L_\beta \end{array}\right]_{3\times 8} \qquad B_{(1)} = \left[\begin{array}{c|c} 0 & 0 \\ \hline (0) & L_\epsilon \end{array}\right]_{3\times 3}$$

where the elements of the partitions are specified by Eqs. (10) and (11). All thrust parameter errors are assumed to be independently derived; thrust-pointing error caused by celestial sensor errors must appear as a common source to all thrusters. Parameter covariance matrices in normalized form are given by the following relations:

$$\Lambda(t,\tau) = \left[\begin{array}{c|c} \mathrm{diag}\left[\sigma_{\dot{x}}^2\right] & (0) \\ \hline (0) & \left[\begin{array}{cc} \sigma_\beta^2 & 0 \\ 0 & \sigma_\beta^2 \end{array}\right] \end{array}\right] e^{-\alpha_x |t-\tau|}$$

$$\Gamma(t,\tau) = \begin{bmatrix} 0 & (0) \\ \hline (0) & \begin{bmatrix} \sigma^2_{\epsilon_y} & 0 \\ 0 & \sigma^2_{\epsilon_x} \end{bmatrix} \end{bmatrix} e^{-\alpha_\epsilon |t-\tau|}$$

where $\sigma^2_{\epsilon_y}$ is the sun sensor variance, and the correlation times of the processes for the thruster parameters are assumed identical without loss of generality in accordance with the data of Table 1. Mapping of Λ and Γ by A and B provides the component autocorrelation functions of percentage variation in total thrust for each of the spatial coordinates (x, y, z);

$$\left.\begin{aligned} R_{w_x}(t,\tau) &= \frac{1}{N}\left[\sigma^2_{I_B} + \sigma^2_{C_\theta} + \frac{1}{4}\sigma^2_{V_B} + \frac{1}{400}\left(\sigma^2_{\eta_1} + \sigma^2_{\eta_2}\right) + \frac{1}{40,000}\sigma^2_{\epsilon}\right] e^{-\alpha_x|t-\tau|} \\ R_{w_y}(t,\tau) &= \frac{1}{N}\sigma^2_{\beta}\, e^{-\alpha_x|t-\tau|} + \sigma^2_{\epsilon_y} \sin^2\psi_\odot\, e^{-\alpha_\epsilon|t-\tau|} \\ R_{w_z}(t,\tau) &= \frac{1}{N}\sigma^2_{\beta}\, e^{-\alpha_x|t-\tau|} + \sigma^2_{\epsilon_y}\, e^{-\alpha_\epsilon|t-\tau|} \end{aligned}\right\} \quad (15)$$

An example of thrust error covariance in the spacecraft y axis, caused by sun-sensor errors, is shown in Fig. 5.

The behavior of the standard deviations for the components of $R_w(t,\tau)$ as a function of time is shown in Fig. 1. This summary is a compilation of Eqs. (15), Table 1, and Fig. 5. Standard deviation σ_{w_x} is directly proportional to $1/\sqrt{N}$ and, hence, follows the power curve. Switching points were calculated based on an 18-kW thrust system with six operating thrusters. Standard deviations $\sigma_{w_{y,z}}$ do not follow the $1/\sqrt{N}$ law directly because of the contributions from $\sigma_{\epsilon_{y,z}}$.

REFERENCES

1. Sage, A. P., Optimum Systems Control, Prentice Hall Publications, Inc., Englewood Cliffs, N. J., 1968.

2. Jordan, J. F., "Orbit Determination for Powered Flight Space Vehicles on Deep Space Missions," Journal of Spacecraft and Rockets, Vol. 6, No. 5, May 1969, pp. 545-550.

3. Kerrisk, D. J., Electric Thrust Subsystem Performance Uncertainties, Personal Communication to K. L. Atkins/D. B. Smith, Jet Propulsion Laboratory, Pasadena, California, November 22, 1971.

4. Crawford, W. E., "Undisturbed Limit Cycle Behavior of the Solar Electric Thrust Vector Control System," JPL Engineering Memorandum, E. M. 344-287 WEC, Jet Propulsion Laboratory, Pasadena, California, October 13, 1970 (JPL internal document).

5. Selected Papers on Noise and Stochastic Processes, N. Wax, ed., Dover Publications, Inc., New York, 1954.

Table 1. Thruster performance summary data

Parameter	Nominal value	Calibration accuracy (% nominal)	A priori process standard deviation	Correlation time	Contribution to $\Delta T/T$	
					Bias, %	Time-varying component, %
I_B	Programmed	±0.5	±1.5%	Weeks	0.5	1.5
V_B	1 - 2 kV	±0.5	±1.0%	Weeks	0.25	0.5
$\cos\theta$	0.96	±2.0	±3.0%	Weeks	2.0	3.0
η_1	0.8 - 0.85	±1.0	±5.0%	Days-weeks	0.02 - 0.05	0.1 - 0.2
η_2	0.04 - 0.07	±20.0	±25.0%	Days-weeks	0.5 - 1.25	0.5 - 1.0
ϵ	0.005	±30.0	±30.0%	Days-weeks	0.15	0.15
$\overline{\beta}$	0.0	--	±2/3°	Months	--	1.2 cross axis

Table 2. Summary of estimated Sun-sensor and star-tracker errors

Sensor	Bias, deg	Drift	
		Standard[a] deviation, deg	Correlation time
(ϵ_1, ϵ_2) Sun sensors	≤0.08	0.17	Days - weeks
(ϵ_3) Star tracker	≤0.05	Negligible	—

[a]Assumes a zero mean uniform distribution between ±0.30 deg.

Table 3. Effects of actuator backlash

Actuator	Backlash, steps	Limit cycle period, min	Limit cycle amplitude, deg
Translator	1	30	0.002
Gimbal 1	0.6	30	0.003
Gimbal 2	6	30	0.03

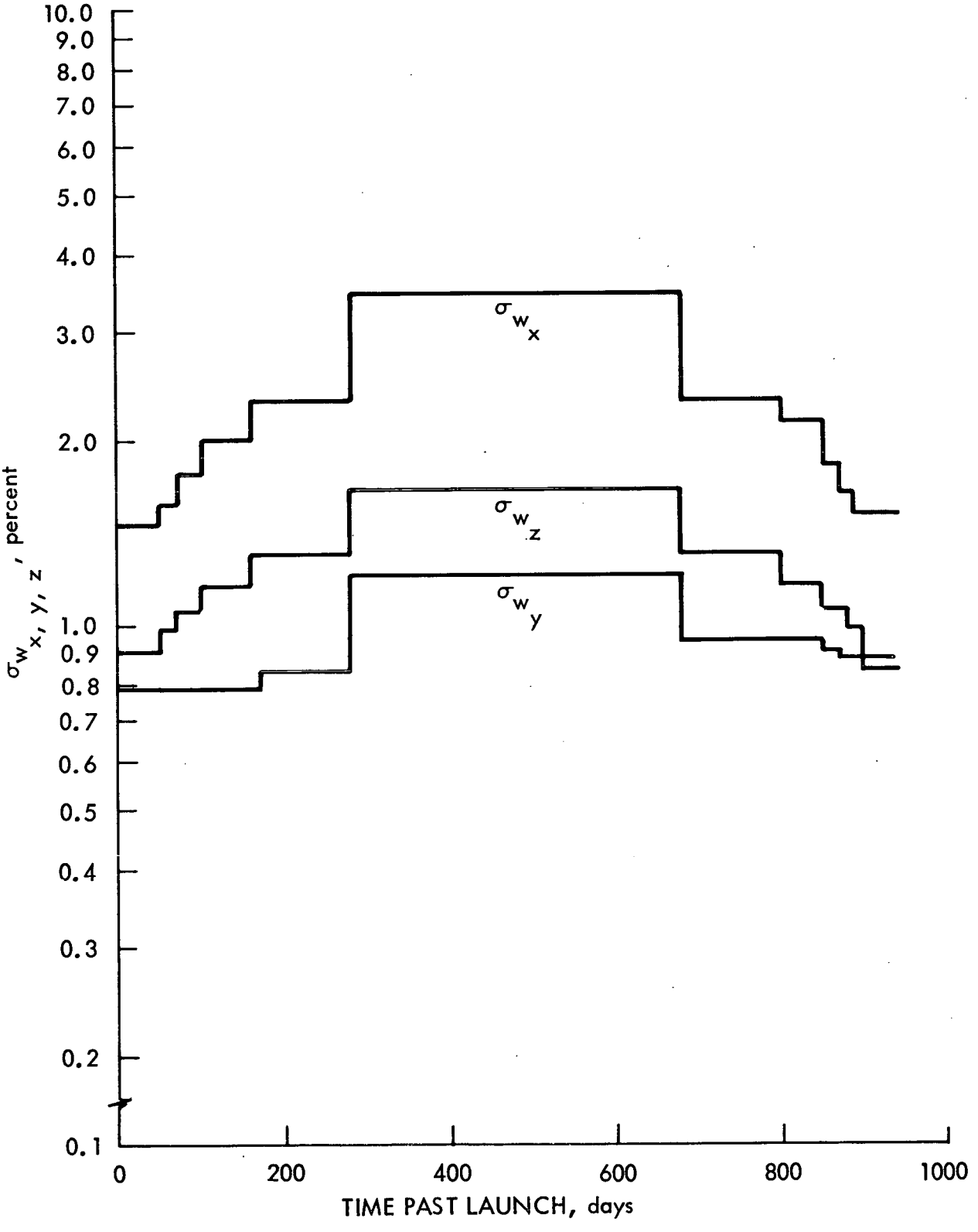

Fig. 1. Standard deviations of component normalized thrust acceleration process noise

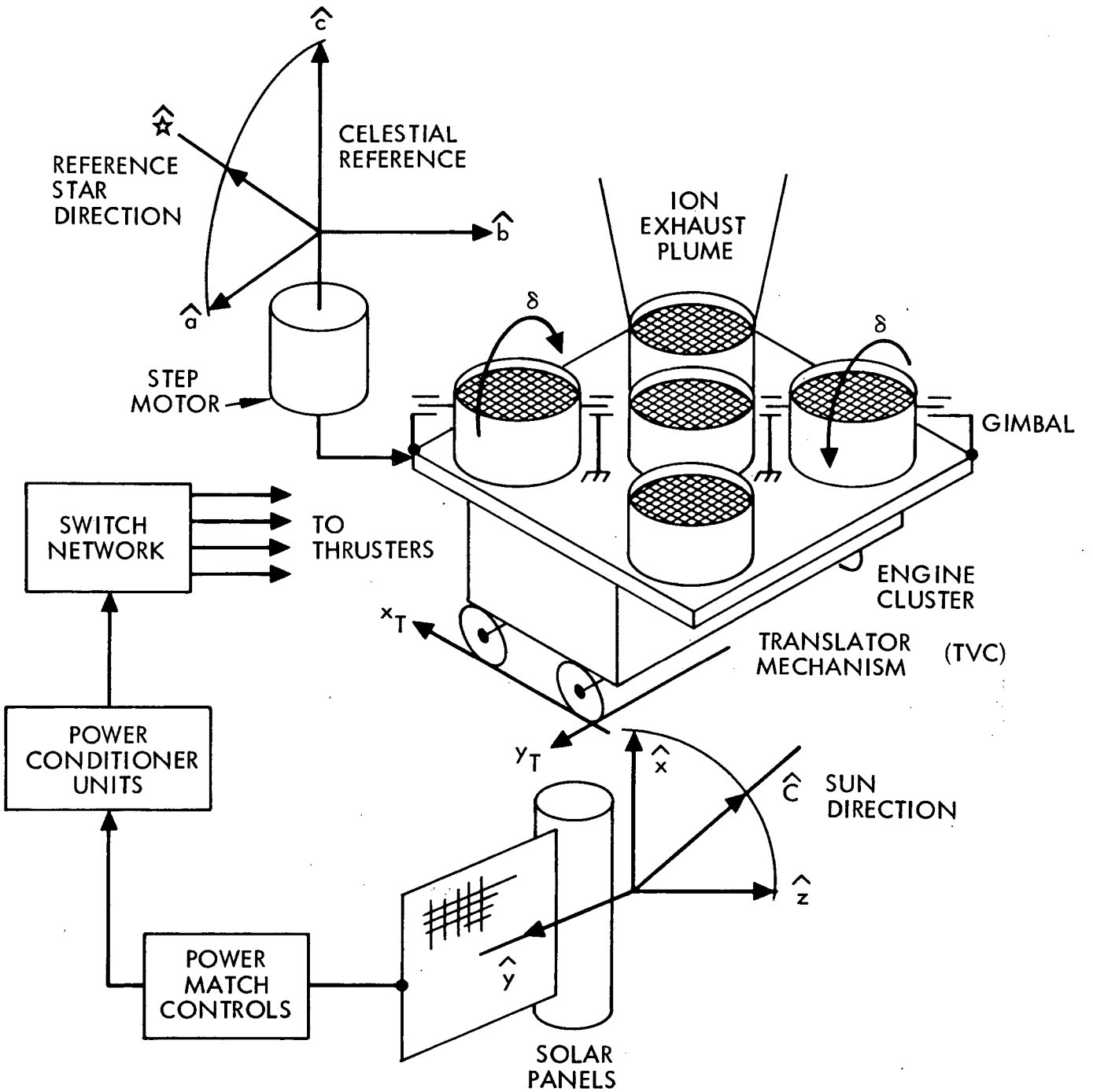

Fig. 2a. Fundamental system functions

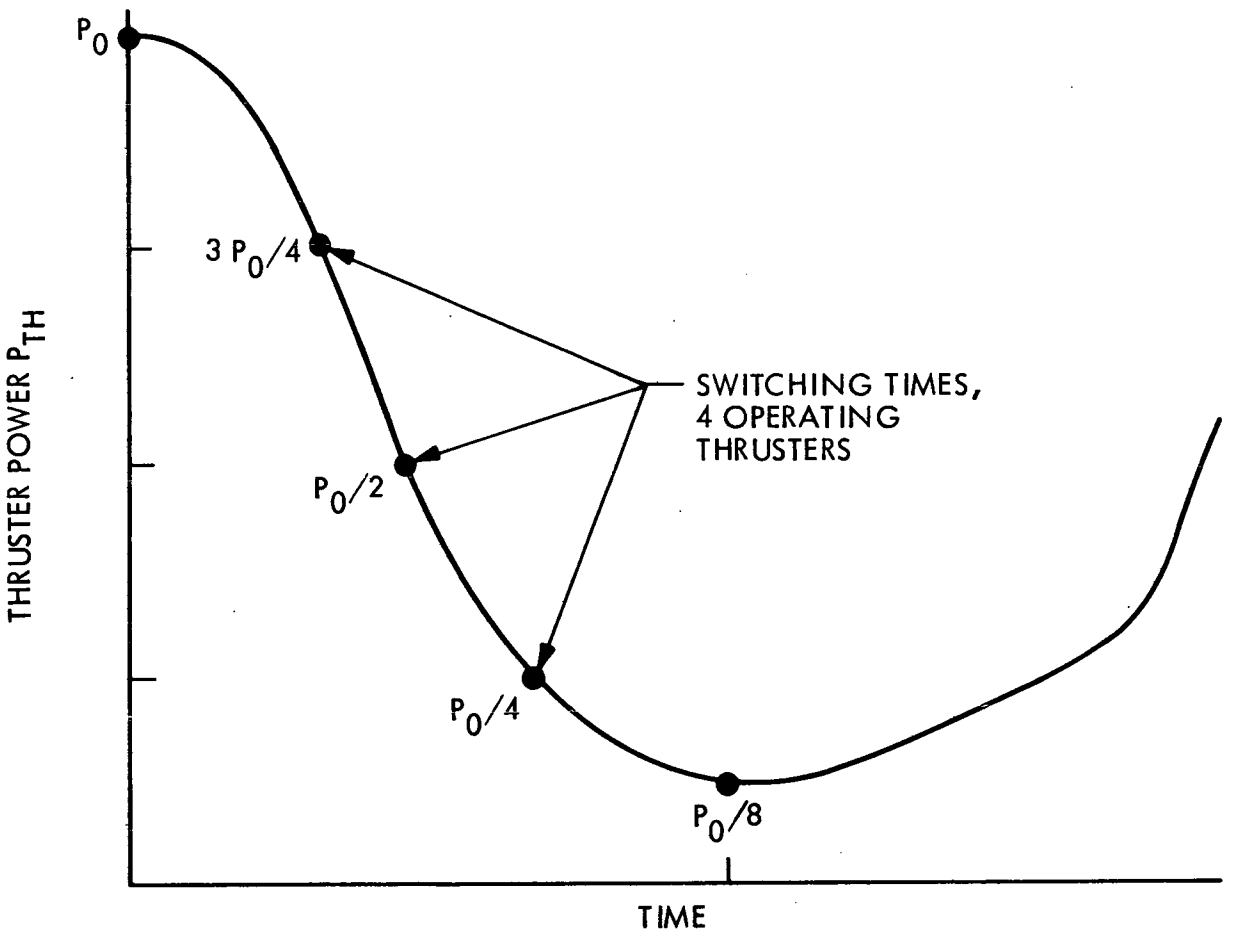

Fig. 2b. Typical power curve and switching strategy

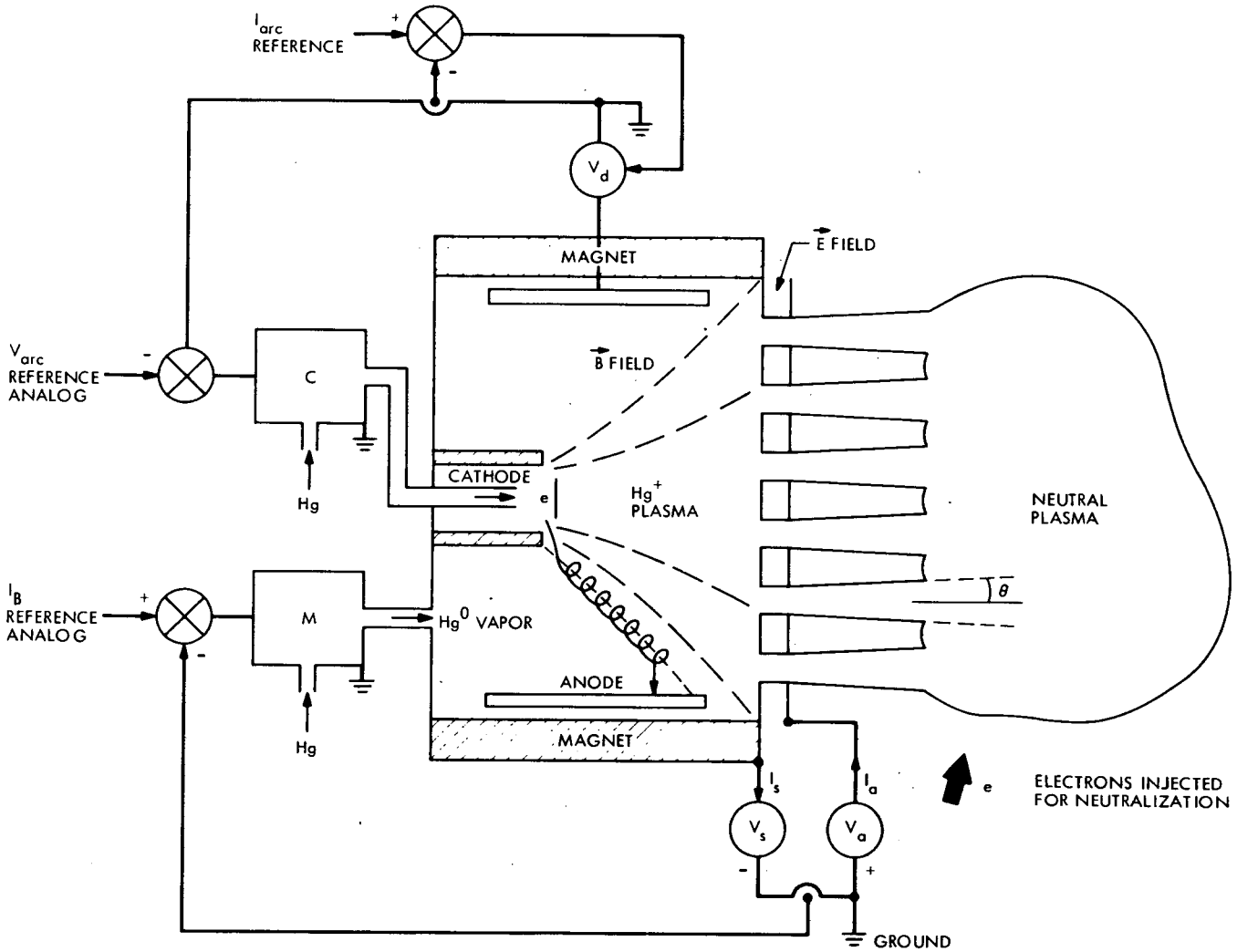

C CATHODE VAPORIZER POWER SUPPLY AND HIGH-VOLTAGE ISOLATOR
M MAIN VAPORIZER POWER SUPPLY AND HIGH-VOLTAGE ISOLATOR
V_s SCREEN (MAIN BEAM) POWER SUPPLY
V_a ACCELERATOR POWER SUPPLY
V_d ARC DISCHARGE POWER SUPPLY
$V_B = V_d + V_s$
$I_B = I_s - I_a$

Fig. 3. Electron bombardment engine (electrostatic thruster)

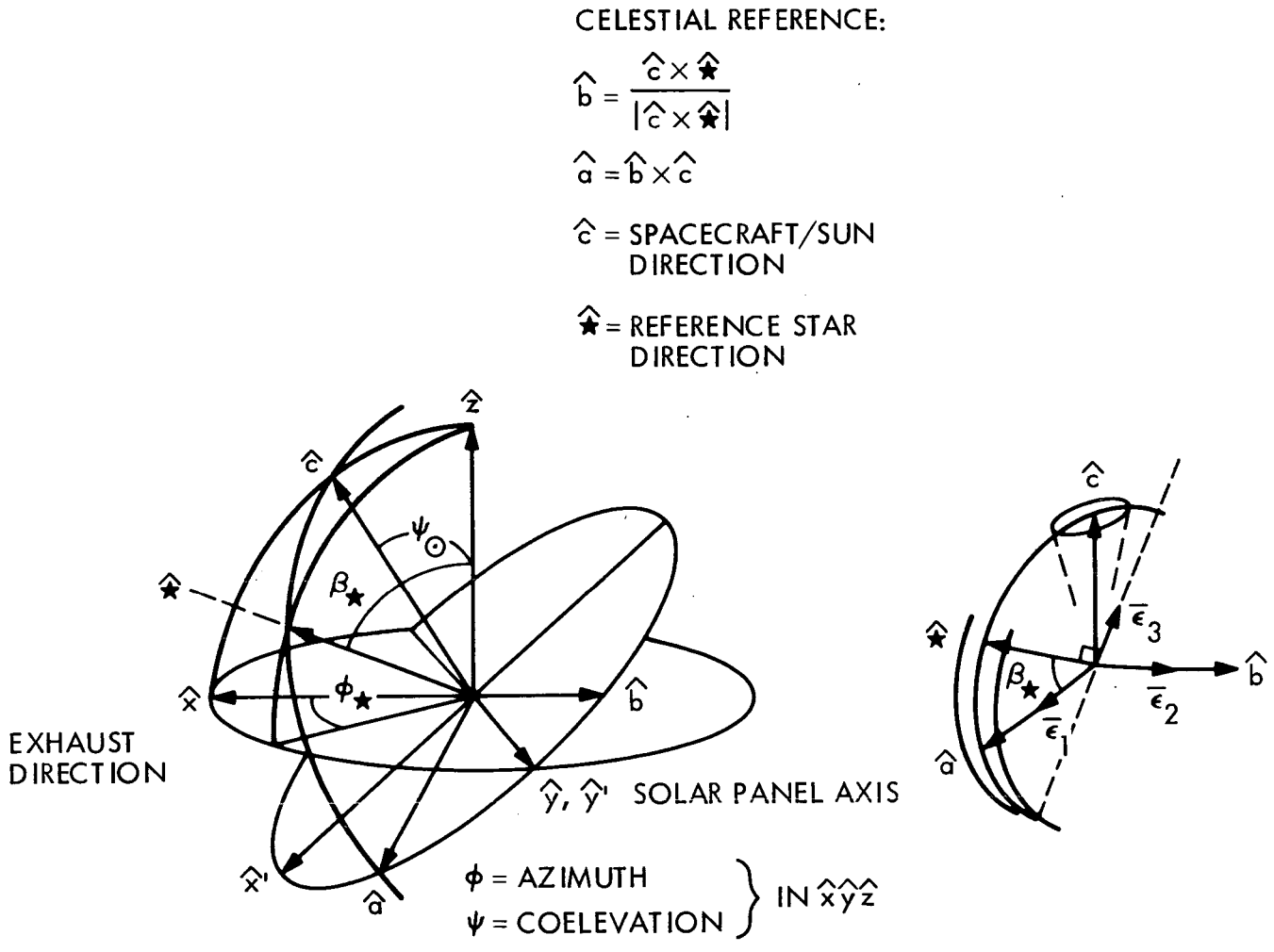

Fig. 4. Celestial and vehicle coordinate system relationships and celestial sensor error definition

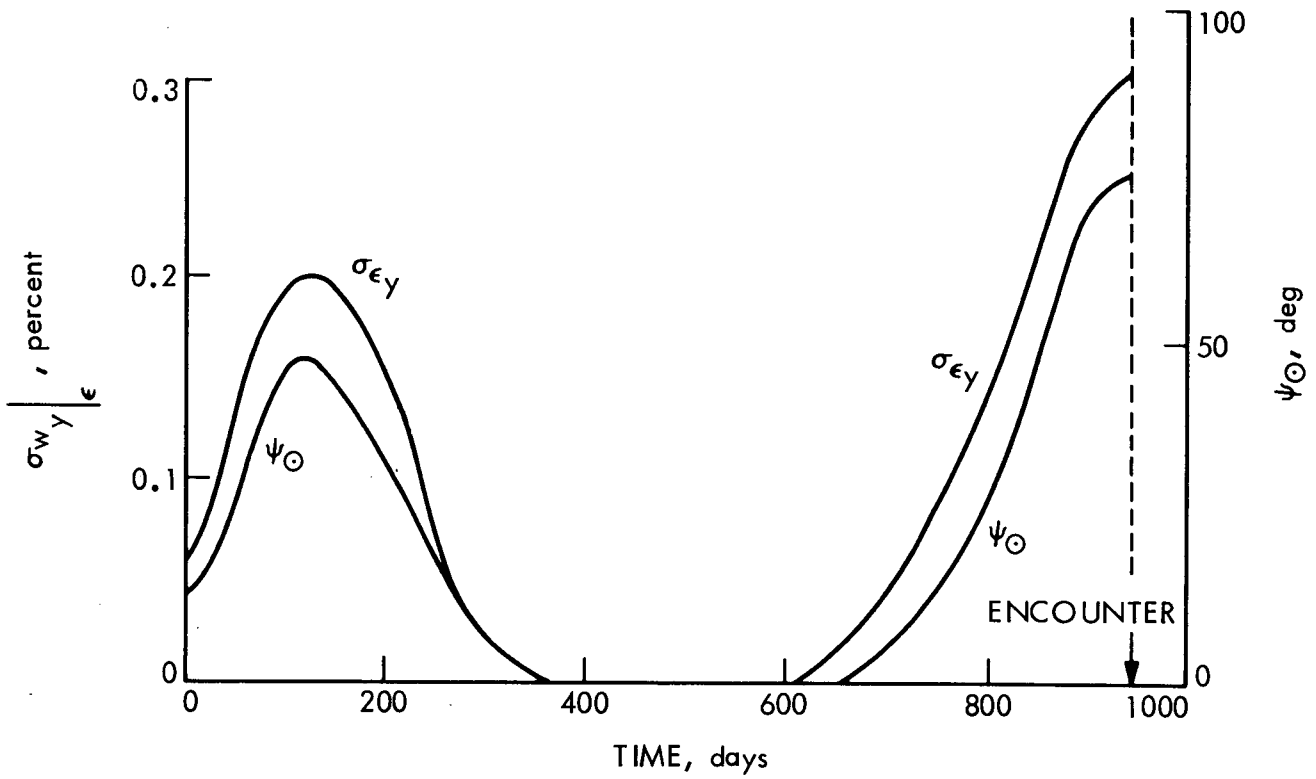

Fig. 5. Thrust error covariance in the spacecraft y axis caused by Sun-sensor errors

APPENDIX A

THRUST EQUATIONS

I. THE ROCKET EQUATION

In some time interval Δt, the impulse imparted to the fluid mass Δm ejected from the rocket (Fig. A-1) must equal the impulse imparted to the rocket. Accordingly,

$$\underbrace{\left[\Delta m\,(\overline{v}_0 - \overline{v}_e) - \Delta m\,\overline{v}_0\right]}_{\text{(Fluid Mass)}} = \underbrace{\left[(m_0 - \Delta m)\,\overline{v}'_0 - (m_0 - \Delta m)\,\overline{v}_0\right]}_{\text{(Rocket)}} \quad \text{(A-1)}$$

Let

$$m(t) = m_0 - \Delta m$$

Use of the impulse-momentum principle in conjunction with Eq. (A-1) provides

$$\overline{T}\,\Delta t = -\Delta m\,\overline{v}_e = m(t)\,(\overline{v}'_0 - \overline{v}_0)$$

Let

$$\Delta t \to dt \quad \text{and} \quad \overline{v}'_0 - \overline{v}_0 \to dv$$

resulting in

$$\overline{T} = -\frac{dm(t)}{dt}\,\overline{v}_e = m(t)\,\frac{d\overline{v}}{dt} \quad \text{(A-2)}$$

II. THRUST EQUATION FOR AN ELECTROSTATIC ENGINE

The absolute magnitude of the total thrust from an electrostatic engine is, from Eq. (A-2),

$$T = \dot{m}\,v_e$$

where v_e is the average velocity of the mercury ions at some exit plane in the exhaust plume, which is composed of thousands of ion beamlets (Fig. A-2). At some time t, let n_0 total ions cross the exit plane where n_1 and n_2 singly and doubly charged ions have velocities v_1 and v_2 such that

$$n_1 + n_2 = n_0$$

The average exhaust velocity is

$$v_e = \frac{n_1}{n_0} v_1 + \frac{n_2}{n_0} v_2 \tag{A-3}$$

The energies associated with the singly and doubly charged ions are

$$\left.\begin{aligned} E_1 &= \tfrac{1}{2} m_0 v_1^2 = eV_B \\ E_2 &= \tfrac{1}{2} m_0 v_2^2 = 2eV_B \end{aligned}\right\} \tag{A-4}$$

where

m_0 = mass of atomic mercury

e = charge on an electron

V_B = accelerating potential

The combination of Eqs. (A-3) and (A-4) gives

$$v_e = (\eta_1 + \sqrt{2}\eta_2)\sqrt{\frac{2eV_B}{m_0}}\,\bar{c}_\theta \tag{A-5}$$

where

$$\eta_1 \approx \frac{n_1}{n_0}, \quad \eta_2 \approx \frac{n_2}{n_0}$$

are the mass utilization efficiencies of singly and doubly charged ions and $\bar{c}_\theta$ is the average value of the cosine of the divergence angle for a single beamlet.

The total mass flow rate is

$$\dot{m} = \dot{m}_1 + \dot{m}_2 + \dot{m}_0 \tag{A-6}$$

where $\dot{m}_0$ is the mass flow rate of the mercury required for the cathode and neutralizer. Define the current in the main beam to be

$$I_B = \frac{e}{m_0}\dot{m}_1 + \frac{2e}{m_0}\dot{m}_2 \tag{A-7}$$

where

$$\left.\begin{aligned} \eta_1 &= \frac{\dot{m}_1}{\dot{m}} \\ \eta_2 &= \frac{\dot{m}_2}{\dot{m}} \end{aligned}\right\} \tag{A-8}$$

Equations (A-6), (A-7), and (A-8) are solved simultaneously to obtain

$$\dot{m} = \frac{m_0}{e}\frac{I_B}{(\eta_1 + 2\eta_2)} \tag{A-9}$$

The combination of Eqs. (A-5) and (A-9) gives the desired result:

$$T = \sqrt{\frac{2m_0}{e}}\left(\frac{\eta_1 + \sqrt{2}\eta_2}{\eta_1 + 2\eta_2}\right) I_B \sqrt{V_B}\,\bar{c}_\theta$$

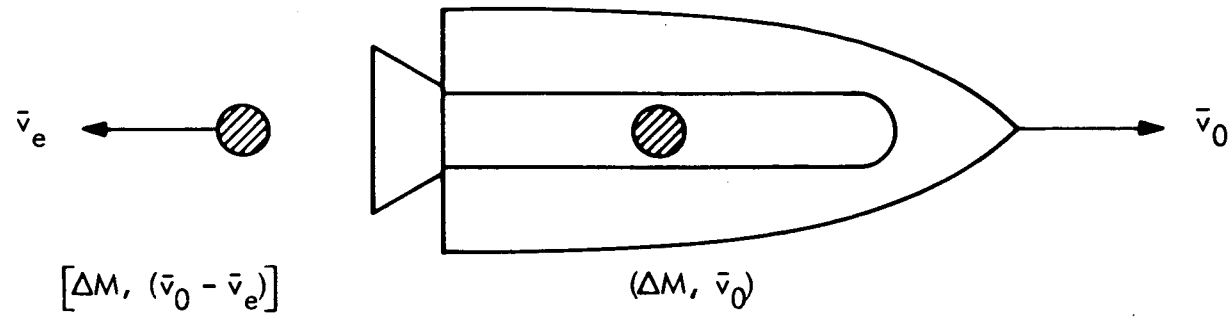

$\bar{v}_e$ EXHAUST VELOCITY OF THE MASS ELEMENT Δm RELATIVE TO THE ROCKET

$\bar{v}_0 - \bar{v}_e$ ABSOLUTE VELOCITY OF THE EXHAUSTED MASS ELEMENT Δm

Fig. A-1. Test rocket for thrust model

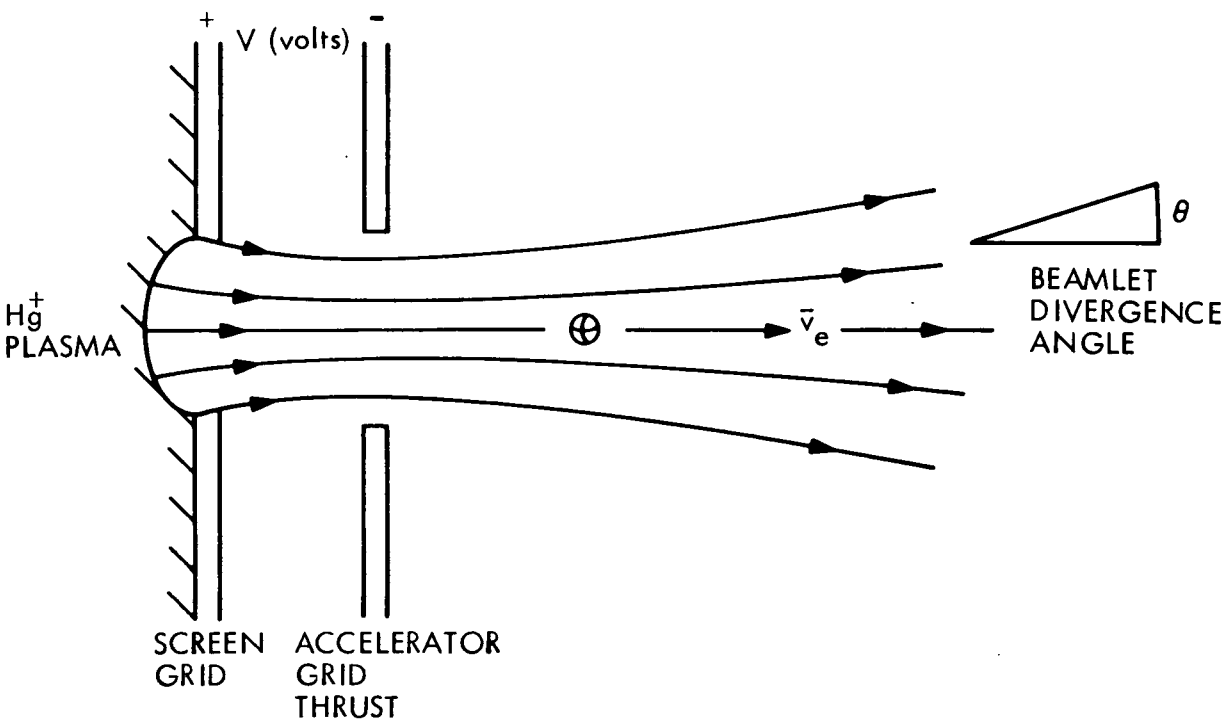

Fig. A-2. Single electrostatic thrust beamlet